

Thermal conditions at the bed of the Laurentide ice sheet in Maine during deglaciation: implications for esker formation

Roger LeB. HOOKE,¹ James FASTOOK²

¹*Department of Earth Sciences and Climate Change Institute, University of Maine, Orono, Maine 04469-5790, USA
E-mail: rhooke@verizon.net*

²*Department of Computer Sciences and Climate Change Institute, University of Maine, Orono, Maine 04469-5790, USA*

ABSTRACT. The University of Maine Ice Sheet Model was used to study basal conditions during retreat of the Laurentide ice sheet in Maine. Within 150 km of the margin, basal melt rates average $\sim 5 \text{ mm a}^{-1}$ during retreat. They decline over the next 100 km, so areas of frozen bed develop in northern Maine during retreat. By integrating the melt rate over the drainage area typically subtended by an esker, we obtained a discharge at the margin of $\sim 1.2 \text{ m}^3 \text{s}^{-1}$. While such a discharge could have moved the material in the Katahdin esker, it was likely too low to build the esker in the time available. Additional water from the glacier surface was required. Temperature gradients in the basal ice increase rapidly with distance from the margin. By conducting upward into the ice all of the additional viscous heat produced by any perturbation that increases the depth of flow in a flat conduit in a distributed drainage system, these gradients inhibit the formation of sharply arched conduits in which an esker can form. This may explain why eskers commonly seem to form near the margin and are typically segmented, with later segments overlapping onto earlier ones.

INTRODUCTION

Many landforms left by continental ice sheets owe their origin to thermal conditions at the glacier bed. Thrust features probably formed in places where the glacier margin was frozen to the substrate but pressure-melting conditions existed a few kilometers up-glacier (Moran and others, 1980). Further inland, at down-flow transitions from a frozen to a thawed bed, higher areas may have remained frozen while lower ones were at the pressure-melting point. Preserved in some of these higher areas are relict periglacial landforms that developed during the last interstadial, such as patterned ground (Kleman and Borgström, 1994) and tors (Kleman and Hättestrand, 1999). Longitudinal compression on the stoss sides of such cold patches may result in stacked transverse moraines; extension in their lee leaves abrupt scarps (Kleman and Borgström, 1994). Drumlins may also be nucleated by such frozen islands (e.g. Patterson and Hooke, 1995, p. 30). At boundaries between zones of thawed and frozen bed, ribbed moraine may form by pull-apart of a once continuous drift sheet (Hättestrand and Kleman, 1999). Finally, the subglacial thermal regime may influence esker formation.

Numerical modeling provides a powerful tool for testing such hypotheses. If the model suggests that there is no possibility of the presumed bed conditions having existed at the appropriate time, alternative explanations for the landforms must be sought. Conversely, to the extent that such hypotheses for the origin of the landforms can be independently verified, the distribution of the features can be used to tune numerical models. Our goal herein is to take a first step towards both of these goals. We tuned the model so that the margin of the model glacier was in certain locations at times that are consistent with field evidence. We then tested it by comparing the predicted basal and mean annual marginal temperatures with those suggested by field data. Finally, we asked what the basal conditions were, how they evolved through time and how they may have contributed to esker development.

THE MODEL

We used the University of Maine Ice Sheet Model, a map-plane vertically integrated finite-element model developed by Fastook (Fastook and Chapman, 1989; Fastook, 1990; Fastook and Prentice, 1994; Johnson, 2002; Johnson and Fastook, 2002). The model can simulate the advance and retreat of the Laurentide and other ice sheets over several glacial cycles. Run in this mode, its output is consistent with that of 15 other ice-sheet models (Huybrechts and others, 1996; Payne and others, 2000). After running the full model for a complete glacial cycle with a coarse grid spacing, one can zoom in on successively smaller areas and run it with much finer grid spacings and a higher time resolution. The earlier solution provides time-dependent boundary conditions for the next (see Appendix A). In our case, we focused on the state of Maine during the period from the Last Glacial Maximum (LGM) to some time before the Younger Dryas.

Climate

As is the case with real ice sheets, the model ice sheet is driven by climate. The $\delta^{18}\text{O}$ record from the Greenland Icecore Project (GRIP) ice core (Dansgaard and others, 1993; Taylor and others, 1993) is used to estimate the temperature in the past at the GRIP drill site (Fig. 1) (Johnsen and others, 1995). At an arbitrary reference point in Maine, the present mean annual temperature is warmer than that at GRIP by an amount ΔT . We refer to this difference as the offset. To generate a proxy record of the temperature distribution over the modeled region in the past, we first add the offset to the GRIP record. Outwards from the reference point we then use present latitude and elevation lapse rates to adjust for geographic location and, in the case of elevation, for the presence of the ice sheet.

From the temperature, we obtain the saturation vapor pressure. Snowfall is then calculated from a correlation between it and saturation vapor pressure (Fastook and Prentice, 1994). Melt rates are based on a positive-degree-day treatment with allowance for daily temperature cycling

across 0°C. In the ablation area, this simple parameterization yields a negative specific mass balance that becomes less negative with increasing elevation. Above the equilibrium line, it yields a positive balance that peaks at the elevation where daily temperature cycles no longer rise above 0°C, and then declines to values typical of a polar plateau at higher elevations. The lapse rates and initial value of the offset are adjusted to yield current mean annual temperatures, as closely as possible (given the limitation of a linear latitudinal lapse rate), within the domain of interest. The latitudinal pole is placed in North Greenland to accommodate the asymmetry of Northern Hemisphere ice sheets.

Finally, the resulting climate is tuned so that, in our case, the ice-sheet margin coincides reasonably well with certain observed marginal positions. Tuning consists of making small changes in the magnitude of the fluctuations in Figure 1 and in the offset.

Ice temperature

Temperatures within and at the base of the ice sheet are calculated based on the mean annual surface temperature, advective effects of ice flow (see Appendix B), strain heating and geothermal flux. The feedback between temperature and ice strain rate is achieved through an iterative process.

In the ablation area, the near-surface ice temperature is likely to be a degree or so warmer than the mean annual atmospheric temperature. This is because the winter snow cover insulates the ice from the deepest winter cold, and percolating meltwater warms the ice before the snow cover disappears in the spring (Hooke and others, 1983). We refer to this difference as $\Delta\theta$. Above the equilibrium line, percolating meltwater can penetrate into permeable firn, releasing the heat of fusion deeper in the glacier. On Barnes Ice Cap, where equilibrium-line temperatures ($\sim -10^\circ\text{C}$) and June snow depths ($\sim 0.5 \text{ m w.e.}$) are comparable to those predicted by our model for the Laurentide in Maine, these processes result in a $\Delta\theta$ of $\sim 2 \text{ K}$ in the ablation area and $\sim 4 \text{ K}$ above the equilibrium line. $\Delta\theta$ decreases rapidly with decreasing temperature (equivalent to increasing elevation). Our model does not take $\Delta\theta$ into consideration, so our near-surface ice temperatures are likely to be too cold in the ablation area and lower part of the accumulation area. Thus, our basal temperature gradients are probably slightly too high, and melt rates too low.

The model also ignores transient changes in heat flux at the ice/bed interface resulting from changes in interface temperature. Between ~ 33 and 29.5 ka (calibrated or calendar years before present; Bronk Ramsey, 1995, 1998) as the ice was making its way into Maine and southwards to the edge of the continental shelf, our model suggests that the mean annual temperature at the margin was $\sim -3^\circ\text{C}$. Thus, the glacier was presumably advancing over thin permafrost. The model predicts that the ice/bed interface would have been near to or at the pressure-melting temperature nearly everywhere in Maine except very close to the margin. Thus, the temperature at the interface would have had to increase $\sim 3^\circ\text{C}$ as the ice advanced over it. We are interested, in particular, in basal conditions after 16.1 ka , so the temperature gradient in the substrate would have had $\sim 13 \text{ kyr}$ to adjust. Calculations using both a theoretical solution by Carslaw and Jaeger (1959, p. 62–63) and a numerical model suggest that the heat flow reaching the interface by that time would have been 99.9% of the long-term average value. Thus, a correction for this transient effect is not necessary.

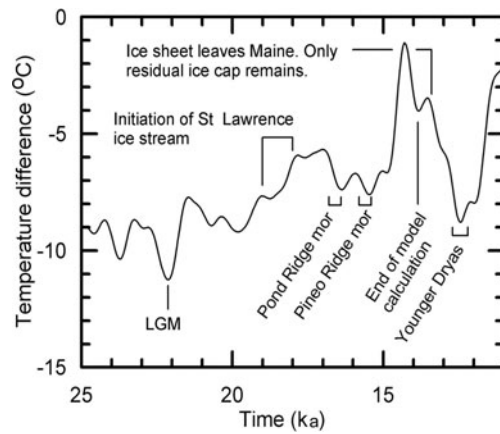


Fig. 1. Temperature record from GRIP in Greenland, used to drive model. The record is expressed in terms of the difference in temperature between the present and the past at GRIP.

Sliding

Because the ice surface slope is low and the bed is generally at the pressure-melting point in our model, over 90% of the surface velocity is a result of sliding. The sliding law used is

$$u_s = C_s(\rho_1 g h \alpha)^p w^q$$

based on that of Weertman (1957b, 1964) modified to incorporate the effect of water at the base of the ice sheet. Here u_s , ρ_1 , g , h , α and w are the sliding speed, density of ice, acceleration due to gravity, ice thickness, surface slope, and amount of available water (including pore-water in the subglacial sediment), respectively, and C_s is Weertman's sliding coefficient. C_s depends on parameters including bed roughness, solute content in the basal ice and rock-to-rock friction, none of which can be known well enough to parameterize independently.

The effect of water on u_s is widely recognized but, as yet, poorly understood. It appears that u_s is dependent both on water pressure, P_w , and on w (Kamb and others, 1994). Beneath ice sheets, P_w is expected to be close to the overburden pressure (Röthlisberger, 1972; Shreve, 1972). Thus, variations in w may have more effect on u_s than variations in P_w .

The basal melt rate is used to calculate w . Longitudinal flow of water along the bed or input of water from the surface are not included. However, C_s and the exponents p and q are chosen to yield velocities that agree with those of measured ice streams and that are consistent with results from a more sophisticated (but computationally more time-consuming) model module that includes longitudinal water flow (Johnson, 2006).

That water might reach the bed of a polar glacier by propagation of water-filled crevasses was predicted theoretically by Glen (1954) and Weertman (1973), but only recently verified by observations (Zwally and others, 2002; Boon and Sharp, 2003). As we do not include this water source in calculating w , we may not adequately capture any down-glacier increase in u_s that occurs where water from the surface first gains access to the bed. We think, however, that this effect is largely smoothed over by tuning, and that the uncertainty introduced is small compared with that resulting from a lack of a rigorous theoretical basis for relating u_s to P_w and w . Furthermore, sensitivity tests described below suggest that the uncertainty in u_s has little effect on our basic conclusions.

Calving

To approximate ice loss by calving at the grounding line, the longitudinal strain rate $\dot{\varepsilon}_{xx}$ is estimated from

$$\dot{\varepsilon}_{xx} = \left(1 - \frac{\rho_i}{\rho_w}\right)^3 \left(\frac{1}{4} \rho_i g h^2\right)^3,$$

where ρ_w is the density of sea water and the ice is assumed to be close to flotation (Weertman, 1957a). Making the approximation that the flow is two-dimensional so $\dot{\varepsilon}_{zz} = -\dot{\varepsilon}_{xx}$, the thinning rate is $\dot{\varepsilon}_{xx}h$. This thinning is added to the (negative) mass balance at the margin. Subsequent comparison with a Brown and others (1982) form of calving law showed little difference between the two approaches. While both accelerated ice loss in the Gulf of Maine, neither resulted in a calving bay migrating up the St Lawrence lowland.

Isostatic adjustment

The model takes isostatic adjustment into consideration, using beam theory to distribute the load of the ice sheet and including a 1/e relaxation time of 3 kyr.

Limitations

The model cannot simulate development of ice streams. The implications of this are discussed in the following section. In addition, the procedure for estimating longitudinal advection of heat is still rather crude. The consequences of this are unknown.

TUNING

In tuning, we tried to adjust the model so that the margin was just offshore of Cape Cod at the LGM (~ 22.0 ka), just inland of the present coast in eastern Maine at ~ 16.1 ka and in north-central Maine at ~ 14 ka. As margin positions were changing rapidly at this time, and are better defined than their ages, we opted to try to match margin positions and let age be a free variable. To achieve satisfactory fits, we increased the offset so the difference in temperature between Greenland and North America was slightly larger relative to today, and we reduced the magnitude of the fluctuations in Figure 1 by $\sim 10\%$. Both are consistent with global climate models that suggest that, due to snow and sea-ice albedo effects, meridional temperature gradients were likely to have been larger during deglaciation than at present (e.g. Rind, 1998).

In Figure 2 we compare margin positions predicted by the tuned model with those based on field data and ^{14}C dates (Borns and others, 2004). We will refer to the Borns and others positions as ‘observed’, recognizing that there is uncertainty in precise locations, in ages, and in temporal correlations.

In drawing their ice margin positions, Borns and others (2004) took into consideration evidence from striations, major topographic elements, end moraines, other ice contact deposits, and detailed local maps. Recognizing the uncertainties in the marine reservoir correction and those resulting from the radiocarbon plateau, and also noting that many dates are minimum estimates of the time of deglaciation, they gave precedence to field evidence where such evidence violated the ^{14}C chronology. In addition, we note that moraines and other ice-marginal indicators are not common in Maine during the time period of interest.

At 17.1 ka, the margin of the model glacier coincides with that observed at 17.3 ka (Fig. 2). Our 16.1 ka margin is slightly too far south in eastern Maine, but our 15.9 ka margin is in good agreement with that observed. In western Maine, both fall between the corresponding observed positions. Our 15.6 ka margin is within 5 km of the mapped position of the 15.6 ka Pineo Ridge moraine in eastern Maine. Our 14.6 ka margin matches that observed in far eastern Maine, but does not show the substantial northward deviation around the Penobscot lowland (PL in Fig. 2) suggested by Borns and others (2004), and is too far north in western Maine. We harbor some doubts about the northern swing of the observed margin around the lowland, as the abrupt turn of the Katahdin esker (KE) to the east, out of the lowland and through a range of low mountains (Fig. 2), is not consistent with a calving bay in the lowland. Our 14.3 ka margin is south of the observed 14.0 ka margin in eastern Maine and north of it in western Maine. In summary, the model glacier appears to reach the coast 100–200 years too late and to retreat too fast in the west and, between 14.6 and 14.3 ka, too slowly in the east. Further tuning might have reduced some of the remaining discrepancies, but experience suggests that our basic conclusions would not be altered.

We attribute the discrepancy in the orientation of the 14.3 ka margin to the inability of our model to simulate the drawdown caused by an ice stream that is believed to have formed between 18 and 19 ka in the St Lawrence lowland to the north (Figs 1 and 2) (Occhietti and others, 2001, p. 259). At ~ 18.4 ka the ice shelf into which this ice stream flowed appears to have broken up, opening a calving bay in the mouth of the St Lawrence estuary. Over the next 3 kyr, this calving bay is thought to have migrated westward and then southwestward up the St Lawrence estuary (Fig. 2). The ice sheet in Maine may have begun to feel the effects of this drawdown as early as 18 ka (Occhietti and others, 2001, fig. 2), but the apparent correlation of the Pineo Ridge moraine with the 15.6 ka cold event suggests that the margin in Maine did not react to the decrease in ice flux across the St Lawrence until later. In due course, however, there presumably would have been a progressive decrease, from east to west, in the flow of ice into Maine. This would have resulted in a more rapid retreat in the east. By 14 ka the residual ice in Maine is believed to have been completely cut off from the rest of the Laurentide ice sheet.

TESTS OF THE MODEL

Margin temperatures at 16 ka

We next compare several estimates of the mean annual temperature at the glacier margin at 16 ka with those predicted by our model. Faunal species in the ice-proximal facies of the Presumpscot Formation suggest arctic to subarctic conditions, with sea temperatures of +1 to -2°C at this time. Oxygen and carbon isotope ratios in the same fauna suggest water of normal salinity with a temperature between 0 and $+2^\circ\text{C}$ (Dorion and others, 2001). To get a sense of the relation between these water temperatures and air temperatures in a modern glacial setting, we compared mean annual sea surface and air temperatures at 68°N off the west coast of Greenland (US National Oceanic and Atmospheric Administration, <http://ferret.pmel.noaa.gov/NVODS/servlets/dataset?catitem=16133>). The two were within a degree of each other, the air being slightly colder.

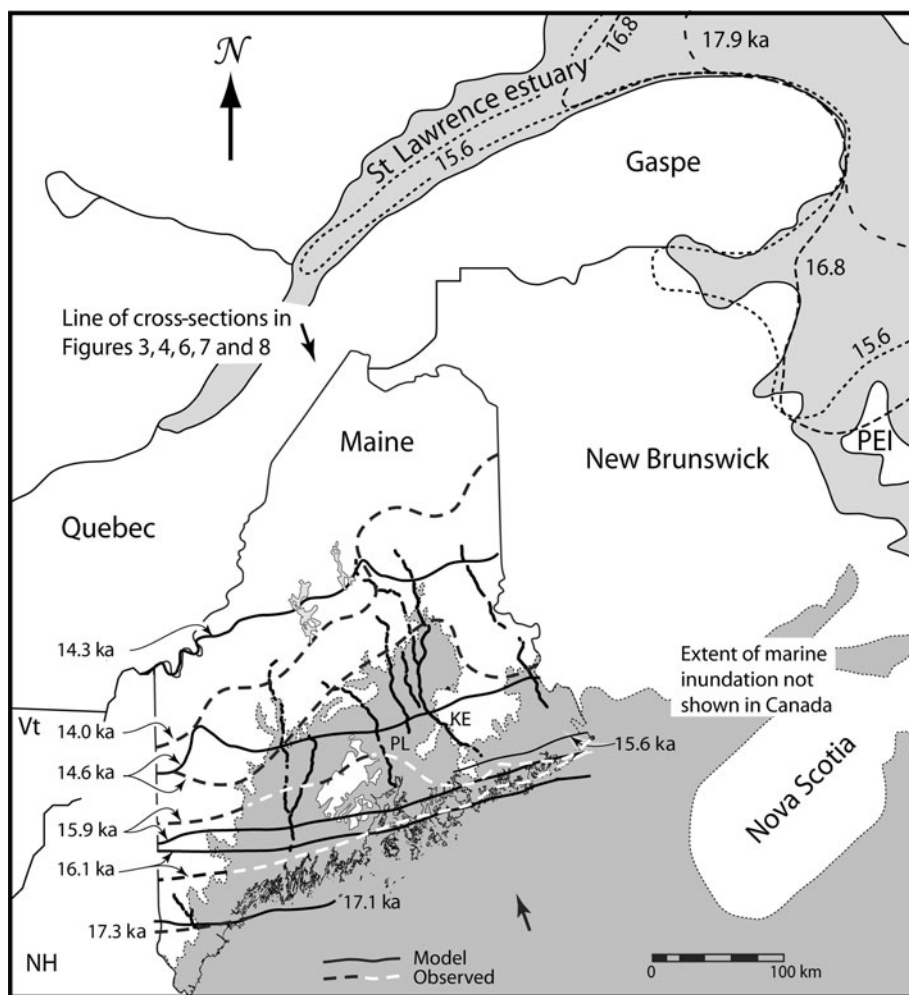


Fig. 2. Location map of Maine (Vt = Vermont; NH = New Hampshire) showing observed (dashed lines) and modeled (solid lines) margins at various times. Also shown are the marine limit (in Maine only), major eskers and Occhietti and others (2001) reconstructions of ice margins in the Gulf of St Lawrence and St Lawrence estuary. KE = Katahdin esker; PL = Penobscot lowland.

Geomorphic data are consistent with these temperatures. Glaciectonic thrust features are common in LGM moraines on Cape Cod, Massachusetts (Oldale and O'Hara, 1984). Moran and others (1980) have argued that such features form where permafrost in the proglacial area extends a distance of 2–3 km under the ice margin so that the bed is frozen there. High pore-water pressures may then result in shear failure at the base of the permafrost. Other features characteristic of permafrost and presumably dating to a time shortly after the LGM are also found in outwash on Cape Cod (Oldale and O'Hara, 1984).

Similarly, Stone and Ashley (1992) and Ashley and others (1999) have found ice-wedge casts and pingo scars in the Connecticut River Valley, ~150 km north of the LGM ice margin. They also describe pollen and macrofossil assemblages from this area that are diagnostic of arctic to subarctic climate with subzero mean annual temperatures. Dates on some of these materials suggest that permafrost conditions persisted here until ~15 ka.

The southern edges of continuous, discontinuous and patchy permafrost in Canada presently roughly coincide with the -8 , -4 and -1°C mean annual temperature isotherms, respectively (Brown, 1970, fig. 3). Thus, we can probably safely assume a mean annual temperature somewhere between 0 and -4°C at the ice margin in Maine at 16 ka.

For comparison, our model gives a mean annual ice-marginal temperature of $\sim -1^{\circ}\text{C}$ at that time. We emphasize that we tuned the model to give this position at ~ 16 ka, but did not tune it to this temperature; this is therefore an independent test of the model.

Basal temperatures

We mentioned earlier several landforms or landform assemblages that are believed to develop when an ice sheet is, at least locally, frozen to the bed. In our model ice sheet, there was only one small frozen area in western Maine at 22 ka, but more had developed by 18 ka and by 15.6 ka the whole northern quarter of the state was frozen (Fig. 3). Owing to the resolution of our model, we could not have detected a narrow frozen margin.

Of the landforms we mentioned, areas of relict periglacial landscape are not known from Maine and, based on our model, would not be expected as there were no areas that remained permanently frozen. However, scattered drumlins are found throughout southern Maine and there is an extensive area mapped as ribbed moraine in the lee of Mount Katahdin (MK in Fig. 3a) (Thompson and Borns, 1985). The drumlins could have been nucleated as the ice advanced, overriding permafrost, or by perturbations other than frozen patches. While we did not find frozen bed

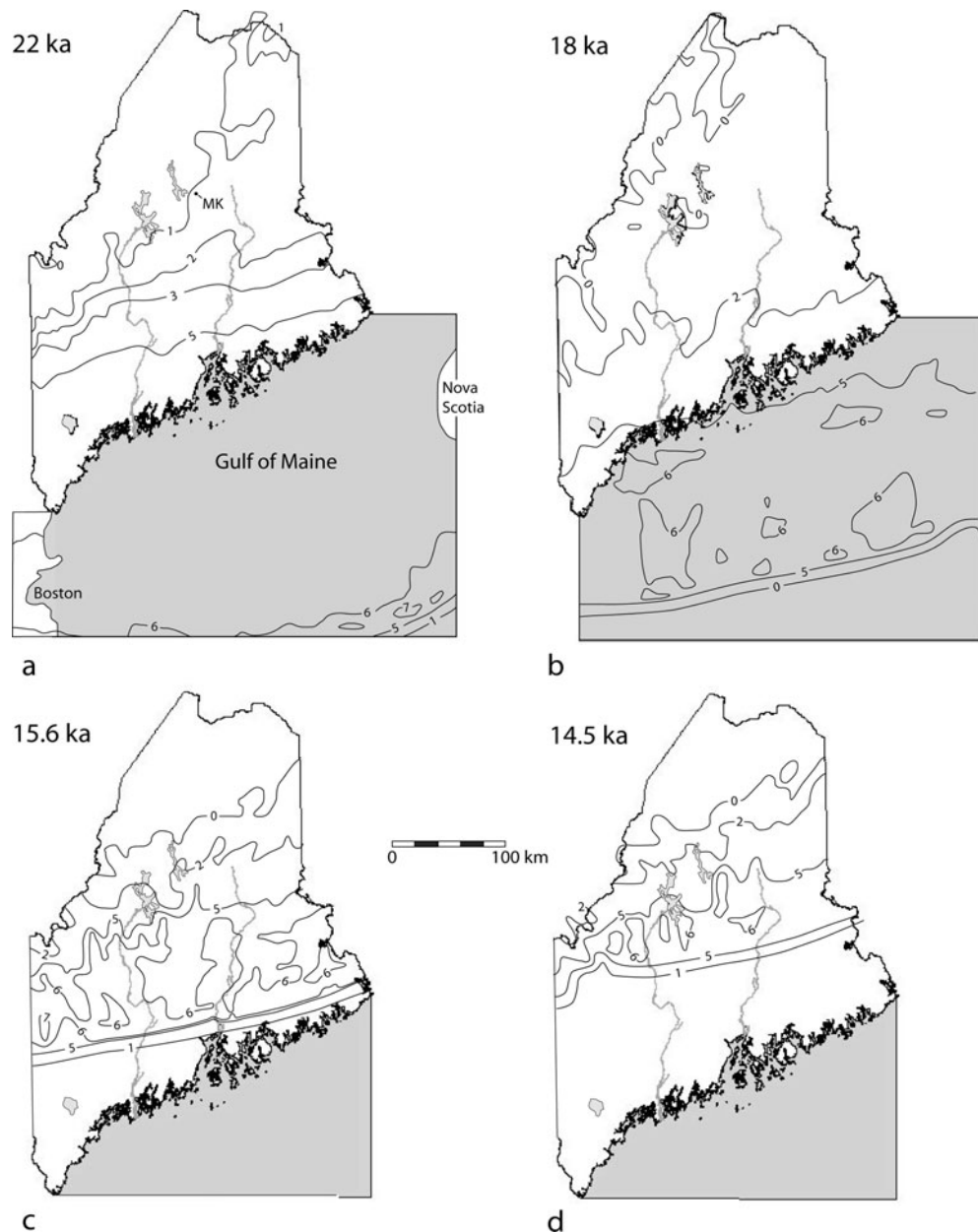


Fig. 3. Maps of basal melt rate at (a) 22.0, (b) 18.0, (c) 15.6, and (d) 14.5 ka. Ice-sheet margin is just south of either the 0 or 1 mm a⁻¹ contour. Lakes shown are, from southwest to northeast, Sebago, Moosehead and Chesuncook. Rivers are the Kennebec (west) and Penobscot (east). MK = Mount Katahdin.

conditions in the area of ribbed moraine south of Mount Katahdin, the melt rate there at 18 ka was <1 mm a⁻¹, so given the uncertainty in the model parameters, particularly in the geothermal flux and longitudinal advection of cold ice, freezing conditions there are well within our limits of uncertainty.

Moraines

It is particularly satisfying that the well-known pause in retreat at the coast at 15.6 ka, resulting in the Pineo Ridge moraine (e.g. Dorion and others, 2001), is reproduced well by our model. This pause is one of two, corresponding to two small cold reversals recorded in the Greenland ice core between 17 and 15 ka (Fig. 1). These pauses show up clearly in an animation of the ice-sheet margin on the computer screen. The earlier pause occurs between 16.5 and 16.3 ka just off the present coast and 24 km seaward of the Pond

Ridge moraine, dated to 16.5 ka (Kaplan, 1999). The ages of these two moraines, although having a resolution of probably no better than ± 200 years, both fall during the cooling phases of the cold reversals. This, rather than the period of maximum cooling, is the time when moraine building would be expected. Of course, we tuned the model to obtain an ice margin just inland from the coast at ~ 16 ka. However, we did not tune the model to obtain moraine-building pauses at these times and locations.

RESULTS

Ice-sheet profiles

Profiles of the ice-sheet bed and surface along an approximate flowline are shown in Figure 4. At the LGM the model bed was depressed ~ 250 m at the present coastline. By 14.25 ka, it had rebounded ~ 50 m.

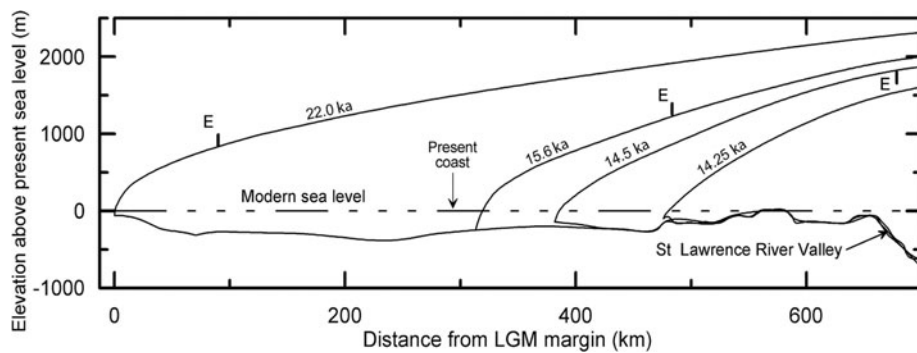


Fig. 4. Cross-sections showing calculated ice-sheet surface and (isostatically depressed) bed topography at various times. Tick marks labeled E show locations of equilibrium lines. Equilibrium line for 14 ka profile is to the right of the diagram. Discrepancies between profiles, particularly along the bed, are a consequence of scaling elevations from computer-generated maps of the bed and surface topography with contour intervals of 75 and 250 m, respectively.

The surface profile of our model ice sheet steepens during retreat. Although contrary to popular conception, this is a logical consequence of an increase in temperature. When the temperature is above freezing, the model assumes that the ablation rate increases linearly with temperature (reaching $\sim 5 \text{ m a}^{-1}$ at the margin at 15.6 ka). In the model, an increase in temperature alone therefore simply increases the daily melt by the same amount everywhere in the ablation area. However, because the number of days with temperatures above 0°C is higher at lower elevations, the increase in annual ablation is significantly larger near the margin. For example, with a mean annual temperature at the margin of $+4^\circ\text{C}$, a sinusoidal annual temperature cycle with a range of 12 K and a lapse rate of -0.006 K m^{-1} , a 1 K increase in mean annual temperature results in an increase in the annual melt rate at the margin which is more than twice the increase at the elevation of the 15.6 ka equilibrium line. The slope of Breiðamerkurjökull in Iceland increased in a similar fashion as it retreated between 1903 and 1998 (Evans and Twigg, 2002, fig. 4).

Field evidence is sometimes interpreted as reflecting a decrease in marginal slope during retreat. Jahns (1953) and Koteff (1974), for example, visualize a marginal zone of thin 'stagnant' ice with a low surface slope bordering active ice. Their marginal zone is only a few kilometers wide and may develop due to accumulation of a moraine cover with a consequent reduction in ablation rate. Although this ice is referred to as stagnant, 'slowly moving' would probably be more accurate. Development of such a zone cannot be simulated with our model, as the spatial scale is less than our $\sim 12 \text{ km}$ grid spacing and we do not have an algorithm for debris content of basal ice.

Basal melt rate

In nature, the basal melt rate m (Figs 3 and 5) is determined by the difference between: (1) the heat reaching the bed from the interior of the Earth (the geothermal flux) plus that generated at the bed by strain heating, and (2) the heat lost by conduction upwards into the ice. The heat produced at the ice/bed interface by strain heating is $c_s \tau u_s$ where c_s is a coefficient of proportionality, τ is the basal traction and u_s is the sliding velocity. The value of c_s depends upon the effective strain rate, the bed slope and the bed roughness. $c_s \tau u_s$ cannot be significantly greater than the potential energy lost as the center of mass of an ice column moves to lower elevations. On a horizontal bed, the potential energy

lost as the center of mass of an ice column decreases in elevation is $\tau u_s / 2$. On the adverse bed slopes that commonly result from isostatic depression of the crust, the decrease in potential energy is still less than this, and some of this energy is dissipated as heat through straining in the ice, including flow around irregularities on the bed. Thus, c_s is generally significantly less than 1/2. In an ice stream, most of the potential energy lost is dissipated in side shear, so $c_s \ll 1/2$. In the model, we use $c_s = 0.1$, but suspect that this may be a little low. We also assume that the geothermal flux is spatially uniform and τ turns out to be nearly uniform. Thus in the model, spatial variations in heat input are largely due to variations in u_s (Fig. 6).

The calculated basal melt rate is 0 at the margin, but rises rapidly to 5–6 mm a^{-1} within a few kilometers (Figs 3 and 5). It then declines gradually for 150 km or so, before beginning a more precipitous decrease. Owing to the uncertainty in c_s , these melt rates may be low.

Basal temperature gradient

The rate at which heat is lost upward into the ice is closely proportional to the basal temperature gradient, β_o . When there is liquid water at the bed, this gradient is determined (both in nature and in the model) by the mean annual temperature at the glacier surface, conduction of heat in the ice, advection of heat by ice flow, strain heating, and transient changes associated with the changing climate. β_o is not output from the model, however. Thus, we calculated it

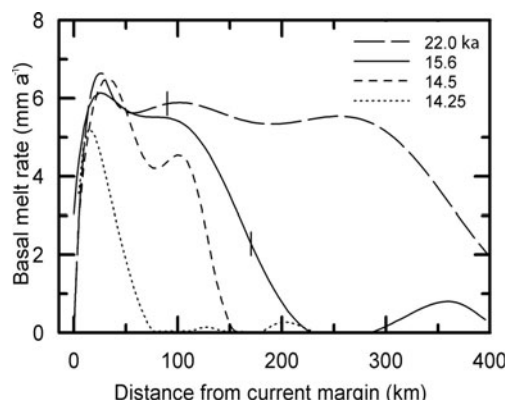


Fig. 5. Basal melt rate at various times as a function of distance from current margin. Tick marks show positions of equilibrium lines.

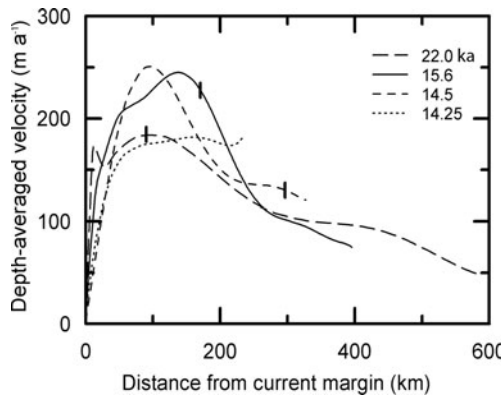


Fig. 6. Depth-averaged velocity at various times as a function of distance from current margin. Tick marks show positions of equilibrium lines.

from the difference between the energy input and that consumed by melting; it is plotted in Figure 7. β_o is largest where the vertical velocity is downward, moving cold ice toward the bed, and where there is appreciable strain heating at the ice/bed interface. Owing to the high sliding speed the vertical velocity is downward throughout the upper half of the ablation area.

At distances greater than about 50 km from the glacier margin, β_o increases dramatically as the ice sheet begins to retreat. There is relatively little change in the spatial pattern of β_o between 15.6 and 14.25 ka; the pattern simply shifts northward with the ice margin. The rapid decline in β_o near the margin contributes to the peak in melt rate there (Fig. 5).

Sensitivity studies

The model parameters to which our results are most sensitive are c_s , the geothermal flux and the enhancement factor in the ice flow law. The latter is the factor by which the ice flow rate is increased over that in pure laboratory ice with a random orientation of c axes. Flow of natural ice is commonly faster owing to development of crystal fabrics with preferred orientations and to the presence of impurities, among other things.

The geothermal flux averages $\sim 50 \text{ mW m}^{-2}$ in Maine (Decker, 1987), and this is the value used in our reference run. For comparison, we ran the model with geothermal fluxes of 40 and 65 mW m^{-2} .

The enhancement factor for our reference run was 8. This is the factor needed to make the volume of ice stored in the Laurentide ice sheet equal to the volume of water lost from the oceans at the LGM and attributable to the Laurentide. We currently estimate this volume to be equivalent to 70 m of sea level. For comparison, we ran the model with an arbitrarily selected enhancement factor of 18.

We did not make runs with different values of c_s because the effect can be estimated reasonably from the other runs.

With increasing geothermal flux, basal melt rates increased (Fig. 8c), resulting in a slight decrease in surface slope and a southward displacement of the 15.6 ka margin (Fig. 8a). Increasing the enhancement factor also resulted in a lower surface profile, compared with the reference run, and in a northward displacement of the margin, apparently due to a reduction in accumulation. The changes imposed resulted in changes in the basal melt rate, averaged over the outermost 200 km of the flowline, of $\sim -17\%$ (enhancement

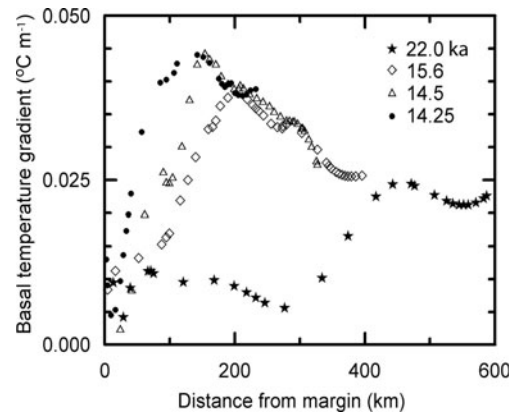


Fig. 7. Temperature gradient in basal ice as a function of distance from the margin.

factor), $\sim -29\%$ (40 mW m^{-2}) and $\sim +40\%$ (65 mW m^{-2}) (Fig. 8b and c). These changes had no appreciable effect on the basal temperature gradient. Our basic conclusions would remain unaltered under any of these scenarios.

DISCUSSION

Two key problems of esker formation can be addressed with the use of our modeling: (1) can eskers be formed in large part, or entirely, by subglacial meltwater? and (2) under what basal thermal conditions do eskers begin to form? First, however, some background will be useful.

Esker physics

A classic paper by Shreve (1972) provides a basis for understanding the paths eskers take. Shreve showed that, deep in a glacier, water should move in a direction normal to planes of equal hydraulic potential in the ice. These planes dip up-glacier at an angle that is ~ 11 times the slope of the glacier surface. At the bed, water flows normal to contours formed by the intersections of the englacial equipotential planes with the subglacial topography. Shreve (1985a, b) shows that this model explains some otherwise puzzling aspects of observed esker paths such as the tendency for eskers to cross divides at their lowest points, and Hooke (2005, p. 232–236) provides some simple examples applying the model.

In an englacial or subglacial conduit, dissipation of energy created by friction in the flowing water melts conduit walls. This is offset by closure of the conduit, driven by a slight difference between the pressure in the water and that in the ice (Röthlisberger, 1972; Shreve, 1972). The latter is approximately equal to the ice overburden pressure. In a steady state, the closure rate and melt rate are equal. Melting of the debris-laden basal ice releases the sediment that forms the esker.

Does surface water reach the bed of a polar ice sheet?

The question of whether or not surface water reaches the bed of a cold ice sheet has been previously problematic. In sufficiently cold ice, the vein system along three-grain intersections (e.g. Raymond and Harrison, 1975) does not become enlarged enough to admit significant amounts of water to the interior of an ice sheet. Many years ago, however, Glen (1954) and Weertman (1973) predicted that

water-filled crevasses would propagate to the glacier bed. Van der Veen (1998) has studied this more recently. Recent field observations support the theoretical prediction. Zwally and others (2002) measured distinct seasonal changes in speed of the Greenland ice sheet at a point near the equilibrium line where the ice is ~ 1200 m thick, the surface temperature is $\sim -11^\circ\text{C}$ (Mock and Weeks, 1966; Wang and others, 2002) and the basal temperature is at the pressure-melting point. The accelerations were in phase with melt rates at the surface. Water reached the bed through scattered moulin. Subsequently, Boon and Sharp (2003) documented propagation of a water-filled crevasse to the bed of John Evans Glacier on Ellesmere Island, Canada, at a point where the 15 m ice temperature was also -11°C and the ice was 150 m thick.

Esker segments

Many eskers, including those in eastern Maine, are believed to have formed in segments (e.g. Donner 1965; Banerjee and McDonald, 1975; Hebrand and Åmark, 1989; Ashley and others, 1991; Bolduc, 1992, p. 115). It is commonly inferred that the segments are built near the distal ends of subglacial drainage systems, and that successive segments form as the ice margin retreats. Left unexplained, however, is why tunnel deposits are not formed in the basal drainage system further up-glacier, or why segments link up as neatly as they do. Banerjee and McDonald (1975, p. 152), for example, concluded that 'subglacial tunnels extend themselves headward as the ice front retreats' but note that 'the details of this extension are unknown'.

On the Katahdin esker in Maine, a typical segment begins as a relatively small ridge. The ridge increases in size down-flow, at first slowly and then more rapidly, resulting in a tadpole shape (Fig. 9). We think the (tadpole) head reflects a period of time during which the margin position was relatively stable, and attribute the non-linear increase in size to: (i) melt rates on conduit walls which increase, thus releasing more sediment, as the glacier surface slope increases near the margin, and (ii) melt rates which exceed closure rates by an increasing amount as the ice thins towards the margin, resulting in a decrease in water velocity and hence in deposition in the tunnel portal. As this part of the Laurentide margin terminated in the sea, finer material that was flushed past the portal was deposited in submarine fans or, where the margin was stable long enough, in deltas. As the margin retreated, successive segments were formed. The head of each younger segment, together with its associated fan or delta, commonly laps onto and buries the tail of the previous one, like shingles. In the Katahdin esker the senior author has identified ~ 30 segments, averaging ~ 5 km in length.

In a meticulous study of the lithologic composition of gravels in several eskers in Labrador, Canada, Bolduc (1992, p. 114–115) found that in some instances vertical variations in pebble lithology were reflected in longitudinal variations along the esker crest. Thus, the lithologic composition of basal beds (and the adjacent till) in one place was similar to that of beds at the esker crest 5–10 km down-flow. She interpreted this as indicating that the same time-stratigraphic unit was being sampled in both places. She then used the shingle analogy to describe how this unit was deposited on the developing esker that increased in height down-flow. Implicit in this interpretation is the assumption that the sediment load at the proximal location at any given time

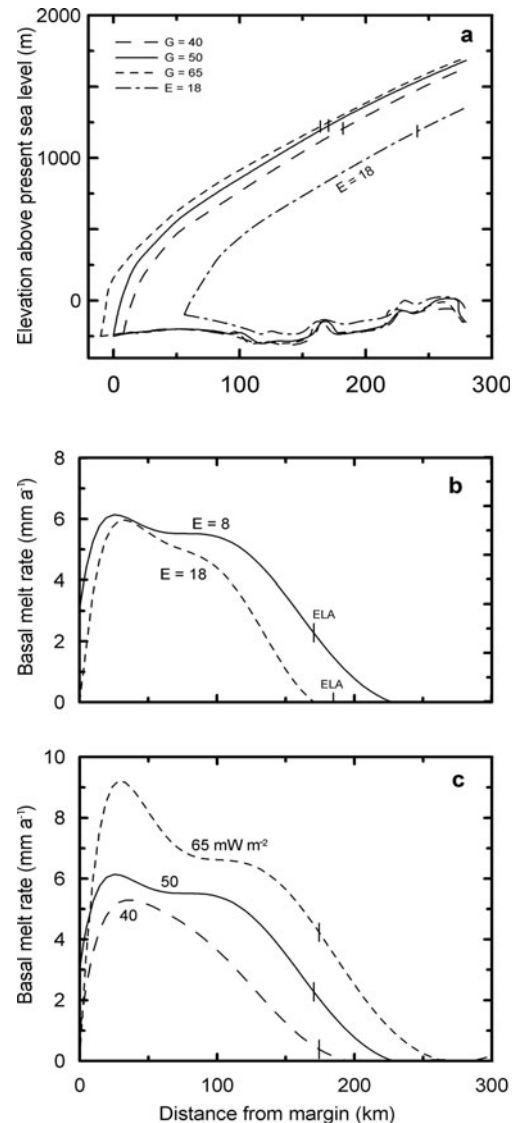


Fig. 8. Sensitivity tests: (a) effect of geothermal flux and enhancement factor on surface profile at 15.6 ka; (b) effect of enhancement factor on basal melt rate at 15.6 ka; and (c) effect of geothermal flux on basal melt rate at 15.6 ka. Tick marks show locations of equilibrium lines.

maintains its identity over the next 5–10 km despite dilution by new material from the tunnel walls and roof. This seems reasonable, in as much as the new material would have been coming from higher in the glacier where sediment concentrations would be lower. Headward growth of the esker along some form of pre-existing subglacial drainage system is implicit in this analogy.

In Bolduc's case, the glacier margin was subaerial and deposition there was in the form of 'flanking aprons' of upward-fining sands and gravels that were, overall, finer than material in the esker. The absence of the 'head' may be due to a less abrupt deceleration of the flow when it emerges subaerially rather than subaqueously.

Shilts (1984, p. 218) thinks that eskers in the Keewatin district, west of Hudson Bay, also grew headward. He suggested that the eskers are a reflection of 'an integrated system of drainage channels developed *on the surface of the glacier*' and that 'meltwater plunge[d] to the base of the glacier to flow in a subglacial tunnel the last few kilometers of its course' (emphasis added). Surface drainage, however,

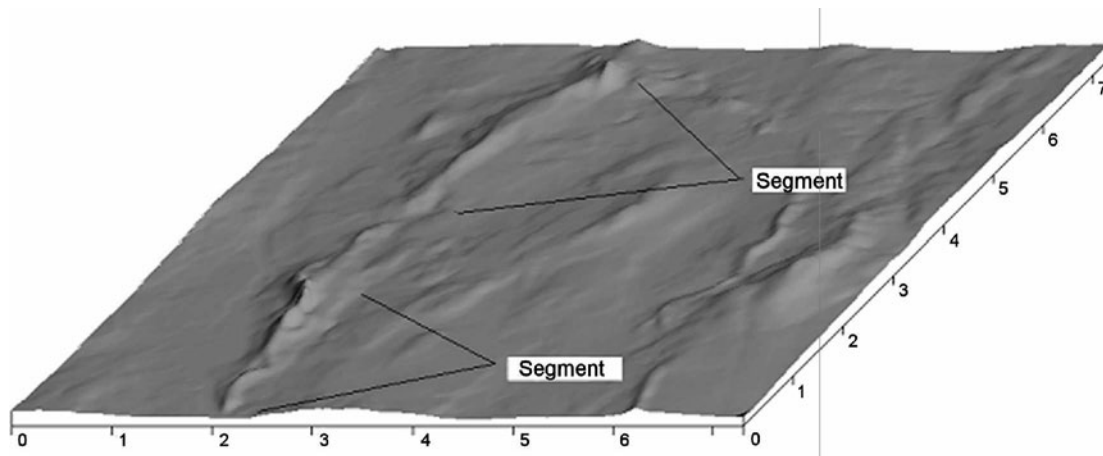


Fig. 9. Oblique view, looking down-glacier, of two segments on the Katahdin esker southeast of Olamon, Maine. Based on a 30 m digital elevation model; scale in kilometers.

would not necessarily follow the course defined by the potential field at the glacier bed, so new moulin would not necessarily form in precisely the right place to result in a continuous esker. Rather, where successive moulin formed in the same subglacial watershed one would expect to see barbs representing situations in which the water reached the bed on the side of a potential valley (Fig. 10). The next segment to develop would then join the earlier one some distance down-flow from the base of the moulin that initiated the earlier segment.

In short, although it is generally agreed that many eskers were built headward in onlapping segments, we have previously not had a satisfactory explanation for how they maintained their continuity as they were extended headward.

Can eskers be built by subglacial meltwater alone?

To address the question of whether eskers can be built by subglacial meltwater alone, we integrated the basal melt rate over the distance from what would probably have been the subglacial drainage divide in northern Maine to the 15.6 ka margin, a distance of ~350 km, and multiplied it by the width of a typical flow band subtended by an esker, ~40 km (Fig. 2). The subglacial drainage divide is judged to have been at the point where the adverse bed slope begins to consistently exceed 1.7 times the surface slope (e.g. Hooke, 2005, p. 249). It is ~80 km north of the present topographic divide (Fig. 4). This integration yielded a discharge at the margin of $1.2 \text{ m}^3 \text{ s}^{-1}$. For comparison, the runs with geothermal fluxes of 40 and 65 mW m^{-2} yielded discharges of 0.8 and $1.7 \text{ m}^3 \text{ s}^{-1}$, respectively. Doubling c_s would have increased the discharge only to $\sim 1.7 \text{ m}^3 \text{ s}^{-1}$.

To estimate the size of material that could be moved by such discharges and the size of a conduit that could carry the flow, we used Parker's (1979) analysis of conditions under which sediment in gravel-bedded rivers is in general motion, adapting it to flow in a semicircular conduit of radius a . The resulting equations are:

$$d_{50} = 2.05 Q^{0.40} S^{0.88} \quad (1)$$

and

$$a = 0.19 \frac{d_{50}}{S}, \quad (2)$$

where d_{50} is the geometric mean particle size in meters, Q is the discharge in $\text{m}^3 \text{ s}^{-1}$, and S is the hydraulic gradient. In these equations, we tacitly assume that the conduit roughness is uniform and comparable to that in gravel-bedded rivers, thus neglecting any difference between the gravel bed and the potentially scalloped ice roof. We also assume that the roughness increases with $d_{50}^{0.2}$ and decreases weakly with Q as in gravel bed rivers. With a horizontal bed, S is well approximated by the surface slope of the ice sheet. Taking S as 0.030, a reasonable mean value within a few kilometers of the margin, it appears that a discharge of $1.2 \text{ m}^3 \text{ s}^{-1}$ could move material with $d_{50} = 100 \text{ mm}$ and would produce a semicircular conduit with a radius of $\sim 0.64 \text{ m}$. Keeping in mind that 50% by weight of the material is smaller than d_{50} and that some of the largest material in the eskers may have simply dropped out of the tunnel roof and not been transported any significant distance, an esker with a d_{50} of 100 mm would be a moderately coarse one. Measurements at three locations on the Katahdin esker yielded estimates of d_{50} of 22, 32 and 46 mm. These measurements were made by passing over 100 kg of material through a set of screens, weighing the material retained on the screens and measuring the long, intermediate and short axes of all material retained on the coarsest (62 mm) screen.

A flow of $1.2 \text{ m}^3 \text{ s}^{-1}$ beneath an ice sheet with a surface slope of 0.030 would melt $\sim 11 \text{ m}$ of ice per year from the walls of the conduit. If the debris content of the ice were 6% by volume, it would take ~ 210 years to accumulate an esker segment 10 m high with 15° side slopes and 25% porosity. This is roughly the average size of the Katahdin esker. The ice front retreated about 120 km between 16 and 14 ka. If it took 210 years to build a segment, only ~ 10 segments could have been built rather than the ~ 25 observed over this distance, and segments would average $\sim 13 \text{ km}$ in length rather than $\sim 5 \text{ km}$ as observed. Furthermore, a 6% sediment concentration is probably the upper limit of likelihood, particularly 10 m above the bed, near the top of a typical esker segment. Thus, it seems that subglacial meltwater alone, although capable of moving the material in the Katahdin esker, is probably not sufficient to build it. Adding superglacial water to bring the total to $6.5 \text{ m}^3 \text{ s}^{-1}$ brings the calculations within reasonable limits. Then, with a 3%

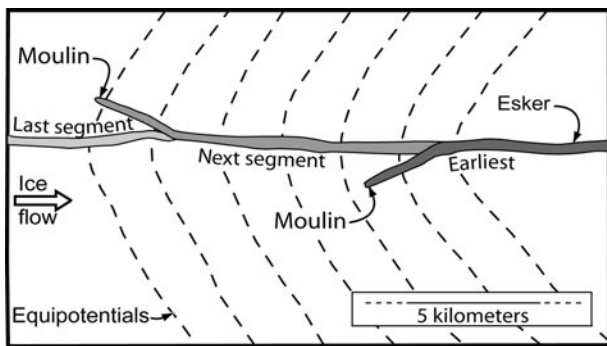


Fig. 10. Plan geometry of a hypothetical segmented esker built by water that reached the bed through moulin. It is assumed that successive moulins are formed as the ice sheet retreats, that the esker begins at the bottom of the moulin and that it subsequently connects with the previously formed segment. Moulins are unlikely to form exactly on the axis of the potential valley. Barbs are therefore expected.

sediment concentration a 5 km segment could accumulate in ~ 80 years, and 25 segments could be built in 2 ka.

However, if surface water was involved, we are faced with the crucial problem mentioned above: why do esker segments line up to form a continuous ridge?

Why do segments line up?

The basal temperature gradient conducts heat upwards into the ice. This reduces the heat available for releasing debris by melting of conduit walls, and thus may play a significant role in determining where eskers begin to form. Consider a situation in which the subglacial water flux is distributed in an anastomosing network of broad low channels occupying a certain fraction f of the glacier bed in a flow band of width w . Noting that the hydraulic radius is one-half the channel depth d , we find from the Gaukler–Manning–Strickler equation that:

$$d = \left(\frac{2^{2/3} n}{f w} \frac{Q}{\sqrt{S}} \right)^{0.6},$$

where n is the Manning friction coefficient. Based on dye trace experiments on Storglaciären, Sweden, we take $n = 0.1 \text{ m}^{-1/3} \text{ s}$ for a shallow subglacial conduit on a rough bed (Seaberg and others, 1988, p. 225). Then, choosing $f = 0.2$, $w = 40 \text{ km}$, integrating the melt rate outward from the divide to obtain Q , and using the surface profile for 15.6 ka in Figure 4 to obtain S , we find that d increases outward from 0 at the subglacial drainage divide to a maximum of $\sim 6 \text{ mm}$, 45 km from the margin. The flow velocity is then $\sim 19 \text{ mm s}^{-1}$. These appear to be reasonable values. Closer to the margin the depth decreases in response to the increasing potential gradient resulting from the increasing surface slope.

Now suppose that the heat dissipated by water flowing in one of the anabranches of this network begins to melt a conduit upwards into the ice, deepening the flow. The increase in discharge in the deeper anabranch will result in an increase in energy dissipation there, and under temperate ice this will result in further melting. Owing to this positive feedback, Shreve (1985a, p. 642) suggested that the resulting conduit would become ‘sharply arched’. The pressure in this conduit will normally be lower than that in smaller

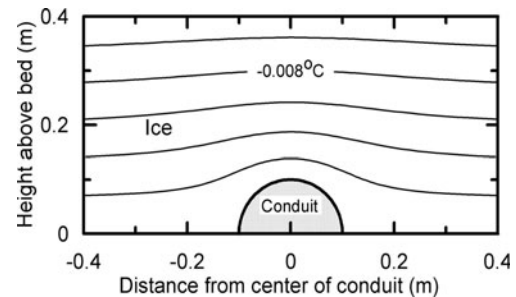


Fig. 11. Calculated temperature distribution in cold ice above a conduit at the pressure-melting point. β_0 is taken to be -0.03 K m^{-1} .

anabranches (Röhlisberger, 1972; Shreve, 1972), creating a tendency for flow from the latter to the former and hence in further enlargement of the developing conduit.

Under cold ice, in situations in which the temperature decreases with height above the bed, the conduit roof must still remain at the pressure-melting point. Thus, the temperature contours immediately above the conduit must be deflected upward relative to those a long distance from it (Fig. 11). Far above the conduit, however, the contours will not be affected. Thus the temperature gradient above the conduit will be higher than elsewhere along the bed, and heat loss from the conduit will be greater. This will inhibit melting of the conduit roof, and hence limit release of debris from the ice. Under suitable conditions, this may prevent formation of an esker.

To partially quantify this argument, consider the temperature distribution around a semicircular conduit (Fig. 11). We ignore advective effects such as flow of ice towards the conduit, and consider only heat conduction. The problem resembles that of flow of an ideal incompressible fluid past a cylinder inasmuch as both involve solutions to the Laplace equation. Adapting a solution to the latter problem (Ablowitz and Fokas, 1997, p. 40–43) yields:

$$T = \beta_0 \left(r - \frac{a^2}{r} \right) \sin \theta, \quad (3)$$

where T is the temperature and r is the radial distance in the direction θ from the center of the conduit. Heat loss through the conduit wall is proportional to the temperature gradient β_a in the ice at $r = a$. From Equation (3),

$$\beta_a = \frac{\partial T}{\partial r} \Big|_{r=a} = 2\beta_0 \sin \theta.$$

Thus, the steady-state heat loss varies sinusoidally from 0 at $\theta = 0$ (parallel to the bed) to twice the average at $\theta = \pi/2$. Over the top of a developing conduit, the heat loss will actually be greater than this because the temperature distribution will not have had time to adjust to the presence of the conduit and because any advection of ice toward the conduit will increase β_a . Thus, while a rigorous analysis would have to treat this as a moving boundary problem and include advective effects, the present steady-state analysis is conservative.

The total heat loss from the conduit in the steady state E_L is:

$$E_L = 2 \int_0^{\pi/2} K_i \beta_a a d\theta = -4K_i \beta_0 a, \quad (4)$$

where K_i is the thermal conductivity of ice. This is twice the heat loss through a planar ice/bed interface of width $2a$,

corresponding to the situation in the absence of the conduit. The minus sign reflects the fact that β_o is negative (because the z axis is positive upwards), so the loss is positive.

Let us now return to the conduit developing in a broad low anabranch of the distributed drainage network. Energy is produced in this conduit by viscous dissipation in the flowing water, E_p , is augmented by geothermal heat, E_g , and is consumed by melting, E_m . Here we neglect: (i) energy dissipated in the water as the water layer is sheared over the bed by the overlying ice, and (ii) energy dissipated by straining in basal ice on either side of the conduit. In a wide, shallow anabranch, the steady-state energy balance is: $E_p + E_g - E_m = E_L$. E_L is proportional to β_o , and β_o is fixed by external factors. E_m is the independent variable, fixed by the values of the three other terms. If the depth of flow in the anabranch is increased slightly by melting of the roof, E_g remains unchanged, E_p increases and as $\beta_o \rightarrow \beta_a$, E_L also increases. If $\beta_o \geq 0$ (ice isothermal or becoming warmer with increasing height above the conduit) or $\Delta E_p > \Delta E_L$, however, E_m will increase and the conduit may then develop a sharply arched form. The question is therefore: when $\beta_o < 0$ how large does an evolving sharply arched conduit (approximated by a semicircular form) have to become before ΔE_p exceeds ΔE_L ? Because the energy loss from a semicircular conduit of radius a is twice that from a broad flat conduit of depth d and width $2a$, we want to know the radius at which E_p is double that of the flat conduit.

At a fixed point on the bed, E_p is proportional to Q (e.g. Hooke, 2005, p. 205–206). Using the Gaukler–Manning–Strickler equation to express Q in terms of the depth d and width $2a$ of the initial sheet flow and radius a of the developing semicircular conduit, we find that the critical radius is:

$$a = 2.82d. \quad (5)$$

Thus, as long as $\beta_o < 0$ in the basal ice, a sheet flow would have to evolve into a semicircular conduit with nearly triple the depth before heat produced in the deeper flow would balance the additional loss.

Uncertainties in this calculation include the effect of bed irregularities, the change in β_o when a flat roof of a broad conduit is perturbed into a more realistic sinusoidal shape, the amount by which β_o would be amplified if the problem were solved as a moving boundary problem and the role of the magnitude of β_o . Nonetheless, we suggest that beneath cold ice this process dampens the tendency for a broad flat conduit to evolve into a sharply arched conduit by melting of the roof. Without such melting, sediment will not be released from the ice and eskers will not form.

Towards the margin, as $\beta_o \rightarrow 0$, the tendency for perturbations to be dampened probably decreases. Among other things, the initial transient amplification of β_a as temperature contours adjust above the conduit will be weaker. We therefore suspect that arched conduits develop before $\beta_o = 0$.

Geomorphic implications

The foregoing analysis applies to an ice sheet resting on a plane bed; esker systems in Maine, however, are located within topography that ranges from undulating hills to low mountains. Furthermore, we have not yet added water from the glacier surface.

We offer the following plausible qualitative scenario. Basal meltwater flows in a distributed system of broad low

conduits throughout most of its journey to the margin. Within a few kilometers or few tens of kilometers of the margin, however, moulins develop by propagation of water-filled crevasses to the bed. Water descending into the moulins encounters a distributed drainage system on a valley side in the potential field at the bed (Fig. 10) and flows down the valley side in this distributed system. In the valley bottom, it joins flow from further up-glacier. As the flow approaches the margin, the magnitude of the temperature gradient in the basal ice decreases until a sharply arched conduit can form. Within the conduit, an esker forms.

Our modeling and calculations suggest that eskers may form only near the margin as further up-glacier temperature gradients in the basal ice prevent the development of arched conduits with melting walls (that supply sediment). Water may therefore reach the bed through moulins further from the margin, but it then spreads out in a distributed drainage system. The correlation between surface melt rates and ice velocity in Greenland (Zwally and others, 2002), for example, suggests the presence of a distributed subglacial drainage system. As arched conduits with lower water pressure begin to develop nearer the margin, water is drawn out of the distributed system into an arborescent system.

This analysis also provides a possible explanation for another interesting characteristic of glacial landforms in eastern Maine. Prior to ~16 ka, water emerging from beneath the ice sheet built submarine ridges of stratified sand and gravel parallel to the margin (Kaplan, 1999). The continuity of these grounding line moraines, their internal structure suggestive of coalescing fans, and their undulating profiles parallel to the margin suggest that the water emerged in many small conduits spaced only hundreds of meters apart (personal communication from H.W. Borns, Jr, 2007). This mode of sedimentation continued during the pause in retreat just inland from the present coast at ~15.6 ka. The huge Pineo Ridge moraine was built at this time. Thereafter, however, moraines ceased to develop; instead, sedimentation took the form of massive eskers. This transition may mark the transition from a distributed drainage maintained by high negative temperature gradients in the basal ice to a more channelized drainage permitted by a wider marginal zone with less negative basal temperature gradients.

To summarize, our calculations (1) suggest that the Katahdin esker was probably not formed entirely by water generated by subglacial melting, and (2) provide a possible explanation for the observation that many eskers are built in segments. The calculations, however, are subject to considerable uncertainty; they support the plausibility of our conceptual model of esker development, but do not prove its validity.

CONCLUSIONS

Our numerical modeling of the retreat of the Laurentide ice sheet in Maine suggests that the ice surface slope may have increased during retreat, that melting conditions obtained over most but not all of the glacier bed in Maine and that the temperature gradient in the basal ice was elevated within 200 km of the margin. Calculations suggest that basal melt rates were not sufficient to produce eskers without additional input of water from the ice surface, and that temperature gradients in the basal ice may have inhibited conduit formation at distances greater than a few kilometers from the glacier margin.

ACKNOWLEDGEMENTS

R.L.H. is indebted to F. Ng for pointing out an error in an early version of Equation (4) and for clarifying other aspects of that solution. Conversations with many people over the years have fueled R.L.H.'s interest in eskers and sharpened his ideas. Deserving special mention is R. Shreve who carefully and exhaustively reviewed three earlier versions of this paper, resulting in many significant improvements (although we apparently have not convinced him that the Laurentide ice sheet in Maine was polar, that the Katahdin esker was built headward in segments, and that the University of Maine Ice Sheet model is up to the task we have given it). We also extend our thanks to J. Kleman and G. Ashley who also constructively criticized earlier drafts, and to W. Warren.

REFERENCES

- Ablowitz, M.J. and A.S. Fokas. 1997. *Complex variables: introduction and applications*. Cambridge, etc., Cambridge University Press.
- Ashley, G.M., J.C. Boothroyd and H.W. Borns, Jr. 1991. Sedimentology of late Pleistocene (Laurentide) deglacial-phase deposits, eastern Maine: an example of a temperate marine-grounded ice-sheet margin. *Geol. Soc. Am. Spec. Pap.* 261, 107–125.
- Ashley, G.M., J.R. Stone and D.M. Peteet. 1999. Chronology and paleoclimate implications from radiocarbon-dated paleobotanical records, Connecticut River Valley, CT. *Geol. Soc. Am. Abstr. Program*, 31(2), A-2.
- Banerjee, I. and B.C. McDonald. 1975. Nature of esker sedimentation. *Soc. Econ. Paleontol. Mineral. Spec. Pub.* 23, 132–154.
- Becker, E.B., G.F. Carey and J.T. Oden. 1981. *Finite elements: an introduction*. Englewood Cliffs, NJ, Prentice-Hall.
- Bolduc, A.M. 1992. The formation of eskers based on their morphology, stratigraphy and lithologic composition, Labrador, Canada. (PhD thesis, Lehigh University.)
- Boon, S. and M. Sharp. 2003. The role of hydrologically-driven ice fracture in drainage system evolution on an Arctic glacier. *Geophys. Res. Lett.*, 30(18), 1916. (10.1029/2003GL018034.)
- Borns, H.W., Jr and 8 others. 2004. The deglaciation of Maine, USA. In Ehlers, J. and P.L. Gibbard, eds. *Quaternary glaciations – extent and chronology, Part II*. Amsterdam, Elsevier, 89–109.
- Bronk Ramsey, C. 1995. Radiocarbon calibration and the analysis of stratigraphy: the OxCal program. *Radiocarbon*, 37(2), 425–430.
- Bronk Ramsey, C. 1998. Probability and dating. *Radiocarbon*, 40(1), 461–474.
- Brown, C.S., M.F. Meier and A. Post. 1982. Calving speed of Alaska tidewater glaciers, with application to Columbia Glacier. *USGS Prof. Pap.* 1258-C.
- Brown, R.J.E. 1970. *Permafrost in Canada: its influence on northern development*. Toronto, Ont., University of Toronto Press.
- Budd, W. 1969. The dynamics of ice masses. *ANARE Sci. Rep.* 108.
- Carslaw, H.S. and J.C. Jaeger. 1959. *Conduction of heat in solids. Second edition*. Oxford, Clarendon Press.
- Dansgaard, W. and 10 others. 1993. Evidence for general instability of past climate from a 250-kyr ice-core record. *Nature*, 364(6434), 218–220.
- Decker, E.R. 1987. Heat flow and basement radioactivity in Maine; first order results and preliminary interpretations. *Geophys. Res. Lett.*, 14(3), 256–259.
- Donner, J.J. 1965. The Quaternary of Finland. In Rankama, K., ed. *The Quaternary*. New York, Interscience, 199–272.
- Dorion, C.C., G.A. Balco, M.R. Kaplan, K.J. Kreutz, J.D. Wright and H.W. Borns, Jr. 2001. Stratigraphy, paleoceanography, chronology, and environment during deglaciation of eastern Maine. *Geol. Soc. Am. Spec. Pap.* 351, 215–242.
- Evans, D.J.A. and D.R. Twigg. 2002. The active temperate glacial landsystem: a model based on Breiðamerkurjökull and Fjallsjökull, Iceland. *Quat. Sci. Rev.*, 21(20–22), 2143–2177.
- Fastook, J.L. 1990. A map-plane finite-element program for ice sheet reconstruction: a steady-state calibration with Antarctica and a reconstruction of the Laurentide ice sheet. In Brown, H.U., ed. *Computer assisted analysis and modelling on the IBM 3090*. White Plains, NY, IBM Scientific and Technical Computing Department, 45–80.
- Fastook, J.L. and J.E. Chapman. 1989. A map-plane finite-element model: three modeling experiments. *J. Glaciol.*, 35(119), 48–52.
- Fastook, J.L. and M. Prentice. 1994. A finite-element model of Antarctica: sensitivity test for meteorological mass-balance relationship. *J. Glaciol.*, 40(134), 167–175.
- Glen, J.W. 1954. The stability of ice-dammed lakes and other water-filled holes in glaciers. *J. Glaciol.*, 2(15), 316–318.
- Hättestrand, C. and J. Kleman. 1999. Ribbed moraine formation. *Quat. Sci. Rev.*, 18(1), 43–61.
- Hebrand, M. and M. Åmark. 1989. Esker formation and glacier dynamics in eastern Skåne and adjacent areas, southern Sweden. *Boreas*, 18(1), 67–81.
- Hooke, R.LeB. 1977. Basal temperatures in polar ice sheets: a qualitative review. *Quat. Res.*, 7(1), 1–13.
- Hooke, R.LeB. 2005. *Principles of glacier mechanics. Second edition*. Upper Saddle River, NJ, Prentice Hall.
- Hooke, R.LeB., J.E. Gould and J. Brzozowski. 1983. Near-surface temperatures near and below the equilibrium line on polar and subpolar glaciers. *Z. Gletscherkd. Glazialgeol.*, 19(1), 1–25.
- Huybrechts, P., T. Payne and the EISMINT Intercomparison Group. 1996. The EISMINT benchmarks for testing ice-sheet models. *Ann. Glaciol.*, 23, 1–12.
- Jahns, R.H. 1953. Surficial geology of the Ayer quadrangle, Massachusetts. *USGS Geol. Quadrangle Map GQ-21*.
- Johnsen, S.J., D. Dahl-Jensen, W. Dansgaard and N.S. Gundestrup. 1995. Greenland paleotemperatures derived from GRIP bore-hole temperature and ice core isotope profiles. *Tellus*, 47B(5), 624–629.
- Johnson, J.V. 2002. A basal water model for ice sheets. (PhD thesis, University of Maine.)
- Johnson, J. and J. Fastook. 2002. Northern Hemisphere glaciation and its sensitivity to basal melt water. *Quat. Int.*, 95–96, 65–74.
- Kamb, B., H. Engelhardt, M.A. Fahnestock, N. Humphrey, M. Meier and D. Stone. 1994. Mechanical and hydrologic basis for the rapid motion of a large tidewater glacier. 2. Interpretation. *J. Geophys. Res.*, 99(B8), 15,231–15,244.
- Kaplan, M.R. 1999. Retreat of a tidewater margin of the Laurentide ice sheet in eastern coastal Maine between ca 14,000 and 13,000 ^{14}C yr. *B.P. Geol. Soc. Am. Bull.*, 111(4), 620–632.
- Kleman, J. and I. Borgström. 1994. Glacial landforms indicative of a partly frozen bed. *J. Glaciol.*, 40(135), 255–264.
- Kleman, J. and C. Hättestrand. 1999. Frozen-bed Fennoscandian and Laurentide ice sheets during the Last Glacial Maximum. *Nature*, 402(6757), 63–66.
- Koteff, C. 1974. The morphologic sequence concept and deglaciation of southern New England. In Coates, D.R., ed. *Glacial geomorphology*. Binghamton, NY, State University of New York, 121–144.
- Mock, S.J. and W.F. Weeks. 1966. The distribution of 10 meter snow temperatures on the Greenland ice sheet. *J. Glaciol.*, 6(43), 23–41.
- Moran, S.R., L. Clayton, R.LeB. Hooke, M.M. Fenton and L.D. Andriashek. 1980. Glacier-bed landforms of the prairie region of North America. *J. Glaciol.*, 25(93), 457–476.
- Occhietti, S., M. Parent, W.W. Shilts, J.-C. Dionne, É. Govare and D. Harmand. 2001. Late Wisconsinan glacial dynamics, deglaciation and marine invasion in southern Quebec. *Geol. Soc. Am. Spec. Pap.* 351, 243–270.
- Oldale, R.N. and C.J. O'Hara. 1984. Glaciotectonic origin of the Massachusetts coastal end moraines and a fluctuating late Wisconsinan ice margin. *Geol. Soc. Am. Bull.*, 95(1), 61–74.

- Parker, G. 1979. Hydraulic geometry of active gravel rivers. *ASCE J. Hydraul. Eng.*, **105**(HY9), 1185–1201.
- Patterson, C.J. and R.LeB. Hooke. 1995. Physical environment of drumlin formation. *J. Glaciol.*, **41**(137), 30–38.
- Payne, A.J. and 10 others. 2000. Results from the EISMINT model intercomparison: the effects of thermomechanical coupling. *J. Glaciol.*, **46**(153), 227–238.
- Raymond, C.F. and W.D. Harrison. 1975. Some observations on the behavior of the liquid and gas phases in temperate glacier ice. *J. Glaciol.*, **14**(71), 213–233.
- Rind, D. 1998. Latitudinal temperature gradients and climate change. *J. Geophys. Res.*, **103**(D6), 5943–5972.
- Röthlisberger, H. 1972. Water pressure in intra- and subglacial channels. *J. Glaciol.*, **11**(62), 177–203.
- Seaberg, S.Z., J.Z. Seaberg, R.LeB. Hooke and D.W. Wiberg. 1988. Character of the englacial and subglacial drainage system in the lower part of the ablation area of Storglaciären, Sweden, as revealed by dye-trace studies. *J. Glaciol.*, **34**(117), 217–227.
- Shultz, W.W. 1984. Esker sedimentation models, Deep Rose Lake map area, District of Keewatin. *Geol. Surv. Can. Cur. Res. Rep.* 84-1B, 217–222.
- Shreve, R.L. 1972. Movement of water in glaciers. *J. Glaciol.*, **11**(62), 205–214.
- Shreve, R.L. 1985a. Esker characteristics in terms of glacier physics, Katahdin esker system, Maine. *Geol. Soc. Am. Bull.*, **96**(5), 639–646.
- Shreve, R.L. 1985b. Late Wisconsin ice-surface profile calculated from esker paths and types, Katahdin esker system, Maine. *Quat. Res.*, **23**(1), 27–37.
- Stone, J.R. and G.M. Ashley. 1992. Ice-wedge casts, pingo scars, and the drainage of glacial lake Hitchcock. In Robinson, P. and J.B. Brady, eds. *Guidebook for field trips in the Connecticut Valley region of Massachusetts and adjacent states (84th Annual Meeting of New England Intercollegiate Geological Conference)*. Amherst, MA, University of Massachusetts, 305–331.
- Taylor, K.C. and 7 others. 1993. The ‘flickering switch’ of Late Pleistocene climate change. *Nature*, **361**(6411), 432–436.
- Thompson, W.B. and H.W. Borns, Jr. 1985. *Surficial geological map of Maine 1:500,000*. Augusta, Maine Geological Survey.
- Van der Veen, C.J. 1998. Fracture mechanics approach to penetration of surface crevasses on glaciers. *Cold Reg. Sci. Technol.*, **27**(1), 31–47.
- Wang, W.L., H.J. Zwally, W. Abdalati and S. Luo. 2002. Modeling of ice flow and internal layers along a flowline through Swiss Camp, West Greenland. *Ann. Glaciol.*, **34**, 303–308.
- Weertman, J. 1957a. Deformation of floating ice shelves. *J. Glaciol.*, **3**(21), 38–42.
- Weertman, J. 1957b. On the sliding of glaciers. *J. Glaciol.*, **3**(21), 33–38.
- Weertman, J. 1964. The theory of glacier sliding. *J. Glaciol.*, **5**(39), 287–303.
- Weertman, J. 1973. Can a water-filled crevasse reach the bottom surface of a glacier? *IASH Publ.* 95 (Symposium at Cambridge 1969 – Hydrology of Glaciers), 139–145.
- Zwally, H.J., W. Abdalati, T. Herring, K. Larson, J. Saba and K. Steffen. 2002. Surface melt-induced acceleration of Greenland ice-sheet flow. *Science*, **297**(5579), 218–222.

APPENDIX A

Interpolation along the boundary of the higher-resolution area uses bilinear spatial and linear temporal interpolation. A higher-resolution embedded node locates the nearest lower-resolution embedding node in each of four quadrants and treats these as corners of a quadrilateral in which standard finite-element method (FEM) machinery, using a bilinear function of the form $V(x, y) = A + Bx + Cy + Dxy$, can be used (Becker and others, 1981). Having found spatially interpolated values for a node at two different times, simple linear interpolation is used to find the value at the required time. The nested grids used in this exercise start with 100 km grid spacing and 25 year time-steps (smaller than necessary) for the whole Laurentide ice sheet, and progress to a regional grid with 35 km spacing and 25 year steps. The final highest-resolution grid for the state of Maine uses a 12 km grid with 5 year time-steps. Since interpolation is only along the margins of the embedded grid, behavior in the interior represents a higher-accuracy representation of the solution. This is not unlike the usual situation in FEM where a variable grid spacing is used to represent a solution with more or less detail in different areas of the domain (see Becker and others, 1981, for details of the convergence of the FEM solution as element size is reduced).

APPENDIX B

The temperature calculation is a one-dimensional time-dependent calculation at each node, with Dirichlet boundary conditions at the top surface and Neumann boundary conditions at the bed (subject to the condition that the bed temperature cannot exceed the pressure-melting point). To include the effects of longitudinal heat advection, we used a modification of an approach suggested by Budd (see Budd, 1969, p. 87, or Hooke, 2005, p. 131–135) in which the longitudinal rate of warming in the ice is approximated by $u_{si}\alpha\lambda$. Here, u_{si} is the part of the horizontal velocity at the surface that is due to internal deformation, α is the surface slope and λ is the lapse rate. (If the horizontal velocity due to sliding is included, impossibly cold internal temperatures are obtained because temperature gradients near the surface increase and supply the heat necessary to obtain the $u_{si}\alpha\lambda$ warming rate (Hooke, 1977, p. 9; 2005, p. 138).) Since sliding velocities are high, our procedure is a relatively crude approximation of reality, but it does have the realistic effect of reducing basal temperatures and melt rates. This warming rate is added to the source term, i.e. the term including internal shear heating (also calculated as a function of depth). Advection acts not like a heat source, but like a sink as it cools.